Proceedings World Geothermal Congress 2015
Melbourne, Australia, 19-25 April 2015

Comparison of Silica and Cation Geothermometers of Bath Hot Springs, Jamaica WI

DeBonne N. Wishart

Mailing address, International Center for Water Resources Management, Central State University, Wilberforce, OH 45384

E-mail address, dwishart@centralstate.edu

Keywords: Geothermometry, Thermal Springs, Geothermal Resources, Saturation Indices, Hydrogeochemistry

ABSTRACT

Solute geothermometers (i.e. silica and cation) for the Bath Mineral hot springs discharged from fissures and fractures at the ground surface in eastern Jamaica were compared to estimate the temperature of the geothermal reservoir. Partial equilibrium exists between aqueous species in the reservoir fluids and the mineral assemblage quartz. The Na-K-Mg Geoindicator by Giggenbach (1988), Na-K geothermometers and the silica geothermometer based on quartz solubility appear to be the most reliable indicators of reservoir temperature. Temperatures estimated using Na-K-Ca geothermometers were either too high or low to be considered reliable. Overestimation of reservoir temperatures by the Na-K-Ca geothermometer may be due to (1) equilibration at conditions that are hotter and deeper than existing areas of mixing and circulation of groundwater and (2) conductive heat loss. Alignment of the hot springs is related to the structural and tectonic setting of a major strike-slip fault-the Plantain Garden Fault. Hydrogeochemical investigations of the hot springs resulted in reliable estimates of reservoir temperatures ranging 80ºC-102ºC at depths of 1-1.8 km. Results indicate that the localized upwelling of low enthalpy geothermal waters at Bath have sufficient heat-generating capacities and warrants further exploration using geophysical techniques and hyperspectral imaging.

1. INTRODUCTION

1.1 Theoretical Basis of Geothermometry

The theoretical basis of geothermometric methods first proposed by Reed et al. (1984) was the thermodynamic calculation of multi-component equilibria of mineral, water, and gas phases to (1) evaluate the equilibrium status of the system; (2) obtain equilibrium temperature in the event that equilibrium exists for a mineral assemblage; and (3) determine whether dilution or degassing (i.e. CO_2, H_2S, etc.) had occurred. Dilution and degassing may impact the estimated temperature of the geothermal reservoir. Continued water-rock interaction and the precipitation of calcium carbonate ($CaCO_3$) are also two of several factors that will result in the departure of the geothermal system from chemical equilibrium. Despite its comprehensiveness, the theoretical basis has not been applied widely in geothermometry as expected as in reality many factors can impact the equilibrium state of the migrating fluid during its accent to the surface. Therefore, geothermometry based on the emergence temperature of the fluid at the surface (sampling point) may not be a true estimate of reservoir geotemperature as thermodynamic conditions are unknown such as the vapor-fraction which is essential to derive accurate reservoir temperatures (Verma, 2000; Verma, 2015). A more practicable approach requires accessibility to down borehole temperature (BHT) measurements in geothermal exploration wells. However, in the event of the unavailability of *in situ* borehole temperature measurements, empirically-derived solute geothermometers may be utilized as proxies for the characterization of a geothermal reservoir. This further aids in estimating the depth of groundwater circulation, based on an understanding of regional tectonics and geothermal gradients.

1.2 Solute Geothermometers

Quantitative solute geothermometers and mixing models can provide information about the probable minimum subsurface temperatures from the analyses of thermal waters or hot springs that are present in a given area. Both cation and silica solubility geothermometers employ empirical equations or models that rely on temperature-dependent chemical reactions for which equilibrium temperatures are important in geothermal resource evaluation. Geothermometers relate to specific mineral-solute reactions as the hot equilibrium temperature is stored in the fluid and reflects the chemical signature of solute concentration (solute ratios). Several assumptions regarding the application of solute geothermometers to hydrothermal fluids are: 1) the mineral species or coexisting compounds and chemical reactions controlling their ratios in the thermal fluids are temperature-dependent at depth; 2) the presence of an adequate supply of constituent minerals in the thermal fluids; 3) re-equilibration has not occurred during ascent, descent, or discharge; 4) there is no mixing, precipitation or dissolution of the fluids; 5) there is rapid rise of thermal water from the reservoir to the surface; and 6) mineral species or compounds have equilibrated with the fluids in the reservoir. Despite that some or all of the above assumptions might be satisfied for every thermal fluid sample, geothermometers are useful in the preliminary evaluation of a geothermal reservoir. Several semi-empirical geothermometric equations for estimation of geothermal reservoir temperatures have been determined on the basis of their cation exchange ratios or the concentration of soluble phases of SiO_2 with concentrations expressed as mg/L, ppm, mg/Kg or mole/Liter. Silica solubility and cation exchange geothermometers (e.g. Na/K, Na-K-Mg, Na-K-Ca, and K^2/Mg) are some of the most widely used solute geothermometers applied to hydrothermal fluids and wells at numerous geothermal fields across the world by numerous researchers over the past three decades. Some of these authors include (Verma 2015; Santoyo and Díaz-Gonzaleź, 2010; Can, 2002; Verma, 2000; Arnórsson, 2000; Verma and Santoya, 1997; Giggenbach, 1988; Nieva and Nieva, 1987; and Fournier and Truesdell, 1979. SolGeo-the solute geothermometers computer program was written and tested by Verma et al. (2008) using geochemical data from several geothermal wells around the world for decades. Dulanya et al. (2010) compared the results of some of the abovementioned silica and cation geothermometers used to estimate reservoir geotemperatures from the hot springs of Malawi. Recent investigations by Spycher et al. (2014); Peiffer et al. (2014); Gherardi and Spycher (2014); and Battistel et al. (2014) have revised or utilized more innovative methods of geothermometry such as a multicomponent approach coupled with numerical optimization and reactive transport modeling (i.e. in some cases) to (1) supplement data using classical geothermometers and (2) evaluate the influence of dilution and mixing on

geothermal fluids in the reservoir temperatures otherwise assumed not occurring with the application of classical geothermometers. However, estimated temperatures of the geothermal reservoir are deemed more dependable if the results from several techniques are in agreement. This paper summarizes the results of (1) comparisons between temperatures calculated using several cation and silica geothermometric equations and (2) the application of a multicomponent geothermometry method using full chemical analyses to compute the saturation indices (log(Q/K) of reservoir minerals over a range of temperatures to estimate the reservoir temperatures for the Bath geothermal system, Jamaica.

2. GEOLOGICAL SETTING

2.1 Synopsis of the Tectonic Evolution of Eastern Jamaica

The Caribbean island of Jamaica is situated within a geologically young and seismically-active fault zone which evolved at the boundary separating the North American Plate and the Caribbean Plate during the Miocene Epoch 23 million years ago. Geochemical and paleomagnetic evidence suggests the Caribbean Plate is the remnant of two separate Cretaceous oceanic terranes: an island arc and an oceanic plateau (Figure 1) that migrated northeastward on the Farallon Plate along major strike-slip faults in the Caribbean basin between the North and South America tectonic plates (Kerr and Tarney, 2005). The Blue Mountain Range is the most seismically-active region on the island with ongoing neotectonic uplift. Most earthquakes occurring in the region are concentrated at depths of 15 to 30 km and are shallow-focus (Wiggins-Grandison, 2003; Wiggins-Grandison, 2005). Fractures and fissures have formed as a result of compressional deformation along the eastern end of a restraining bend on the Plantain Garden Fault (PGF) in Figure 2. The PGF forms an intraplate, left-lateral strike-slip boundary and the restraining bend that consists of an uplifted region in eastern Jamaica that is bounded at its southern edge by the Enriquillo-Plantain Garden fault (Mann et al. 2007).

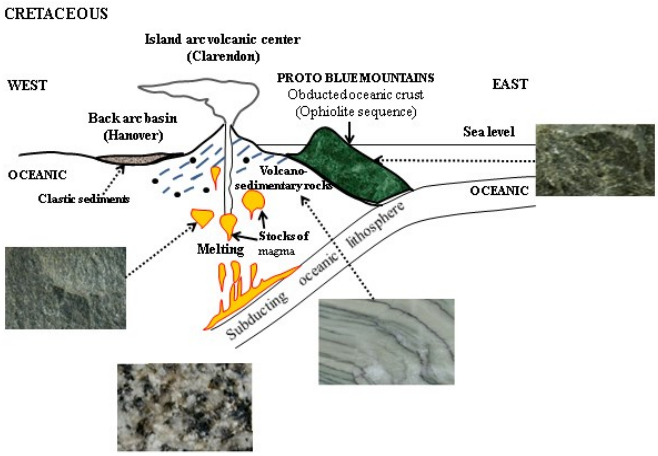

Figure 1: Schematic of the tectonic evolution of the island of Jamaica showing the collision of an oceanic plateau (west) and an island arc (east) to form the Blue Mountains. [Schematic was modified after S. Bhalai, Mines and Geology Division Jamaica.].

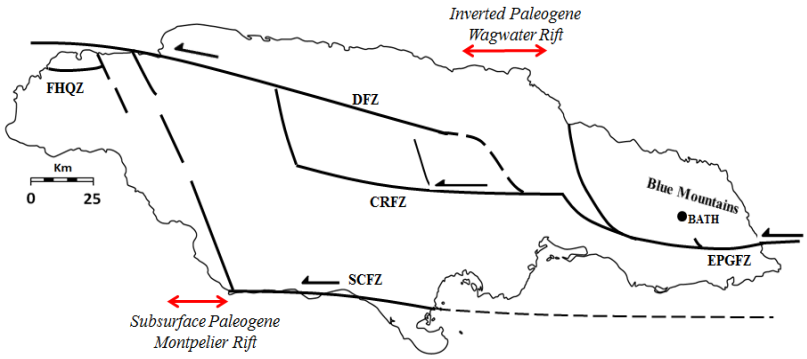

Figure 2: Tectonic map of Jamaica showing major mapped faults on land (Mann et al. 1985) and the offshore Paleocene–Early Eocene rift features in Jamaica associated with the east–west opening of the Early Eocene oceanic Cayman Trough. EPDFZ = Fault Zone; SCFZ = South Coast Fault Zone; CRFZ = Crawle River Fault Zone; FHQZ = Zone, and the DFZ = Duanvale Fault Zone. [This diagram was modified after Mann et al. (2007)].

2.2 Geology and the Occurrence of Bath Springs

The town of Bath (Figure 3) is situated in the eastern parish of St. Thomas, Jamaica and lies within the Blue Mountain Inlier. The Bath hot springs (BTHN, BTHS) emerge from fractures and fissures dissecting a brittle fault zone in Late Cretaceous age suites of massive thoeliitic basalt (i.e. Bath-Dunrobin Basalt) intercalated with tuffs and overlain by a succession of thick, deep marine

shales (Hastie et al. 2008; Hastie et al. 2010). The Bath-Dunrobin Basalt is succeeded by the deposition of the deep-marine Bath Limestone and the Cross Pass Shale. A sedimentary succession located north of the Plantain Garden Fault has been strongly deformed from the duplexing of sedimentary successions by a series of faults. Brittle faults and fissures enhance preferential fluid flow and exert primary control on the development of Bath hot springs in that they provide conduits for the rapid emergence of hot water at depth to the surface at temperatures ranging 50°C – 51.3°C before losing heat. Several springs lie in close proximity (<100m) to each other are considered a single geothermal system. The occurrence of thermal springs here are associated with magmatic activity and heat flow. These hot, boiling springs lie 9 meters above the present level of the east side of the Sulfur River gorge (Hylton, 1987). The largest of several cold springs (BTHC) surfaces from permeable rocks located 18 m above the Sulfur River Gorge and the emerging hot springs.

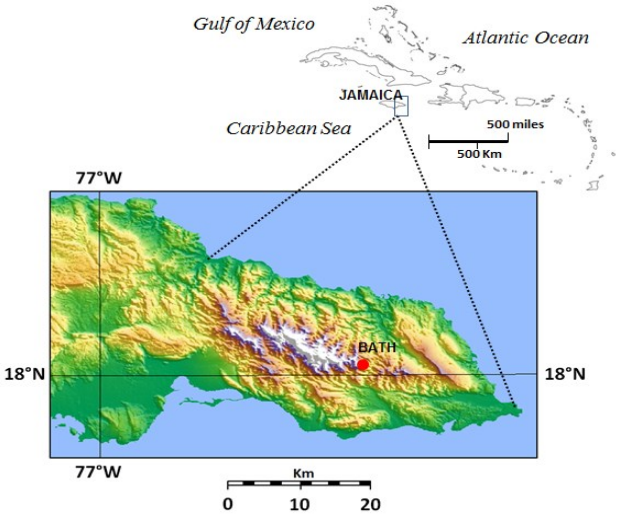

Figure 3: Map of eastern Jamaica showing location Bath and the study region of Bath springs.

3. HYDROGEOCHEMISTRY

The Bath hot spring waters samples (BTHN and BTHS) are characterized as Na-Cl-SO_4 type (Figure 4) with alkaline pH (8.76-8.82) and negative ORP values of -99 mV (Wishart, 2013). The dominant cation and anion order of waters from the hot springs (BTHN, and BTHS) are $Na^+K^+>Ca^{2+}>Mg^{2+}$ and $Cl^->SO_4^{2-}>HCO_3^-$ whereas cation and orders for the cold sample (BTHC) are $Ca^{2+}>Na^+K^+>Mg^{2+}$ and $HCO_3^->Cl^->SO_4^{2-}$ (Figure 5). BTHC is classified as a Ca-Na-Mg-HCO_3 type water. The sulfide (HS^-) concentration of the hot spring is 0.094 mg/L. Negative values for oxidation reduction potential (ORP) observed for the hot spring waters are suggestive of reducing conditions at depth and probable loss of oxygen during the convection of fluids and the reduction of H_2S. Reducing conditions may also have developed at depth due to the oxidation of sulfide (in H_2S) present in alkali chloride waters that forms bisulfate (HSO_4) during buffer action and neutralization of the wall rocks (Ellis and Mahon, 1977). H_2S could also be the result of past volcanic activity associated with the island arc.

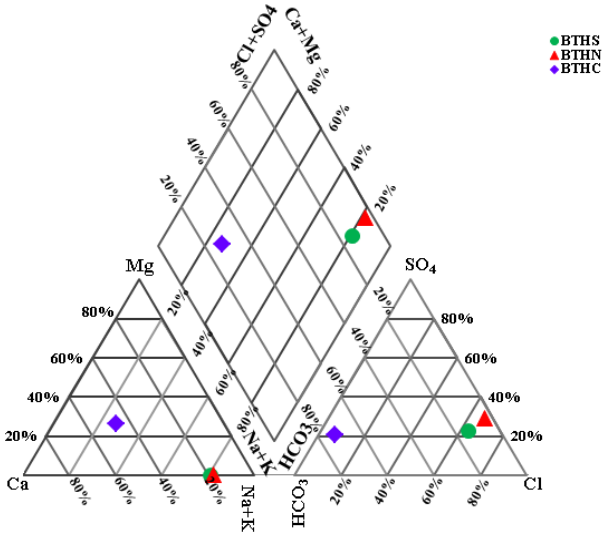

Figure 4: Piper trilinear diagram (1944) of waters for the Bath hot and cold mineral springs, Jamaica showing mixing trends in the waters. [Modeled using AquaChem software].

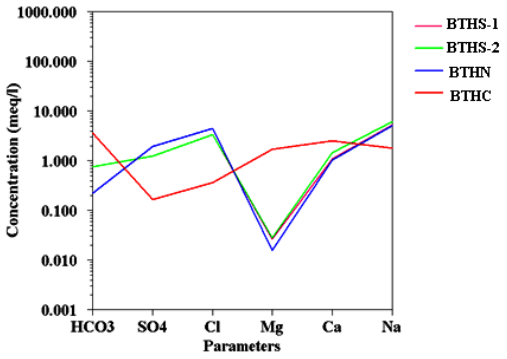

Figure 5: Schoeller (1963) plot of the thermal waters at Bath, St. Thomas, Jamaica. [Modeled using AquaChem software].

4. METHODOLOGY

4.1 Water Sampling and Analysis

Water samples were collected from both hot and cold springs over a course of a year. Physiochemical parameters (i.e. temperature, pH, conductivity (EC), total dissolved solids (TDS), oxidation reduction potential (ORP), and dissolved salinity) were measured *in situ* using electrical meters. Water samples for cation and strontium (Sr) isotope analysis were collected by immersing amber glass bottles at points of emission and sealed and stored in pre-cleaned high density polyethylene (HDPE) bottles with 1:1 nitric acid (HNO_3) preservative to prevent bioalteration. Thirteen pre-cleaned HDPE bottles of un-acidified water samples were collected for anion determination. The samples were stored at 4˚C to the point of lab submission. A total of 42 parameters were determined including physiochemical measurements and major ions (Ca^{2+}, Mg^{2+}, Na^{+}, K^{+}, HCO_3^{-}, SO_4^{2-}, Cl^{-}), trace metals (Li^{+}, Al^{3+}, Ag^{+}, As^{3+}, B^{3+}, Cd^{2+}, Cs^{+}, Cu^{2+}, Fe^{2+}, Mn^{2+}, Pb^{2+}, Si^{4+}, Sr^{2+}, Rb^{+}, Zn^{2+}, Br^{-}, F^{-}, HS^{-}, CO_3^{2-}, NO_2^{-}, NO_3^{-}, SiO_2, PO_4^{3-},and isotopes (Ra^{226}, Ra^{228}, O^{16}, O^{18}, deuterium (δ^2H),and tritium (δ^3H). The flow rate of the samples is 3 L/sec.

4.2 Solute Geothermometry

A common practice for the application of geothermometric equations is to calculate and compare geotemperature estimates from different cation and silica geothermometers. Equations for cation and silica geothermometers used (1) to estimate temperature conditions of the Bath geothermal reservoir and for (2) comparison are listed in Tables 1-3. The concentration of major cations and silica in solution is a function of the temperature, pressure and the length of time between the reaction of the fluid and the reservoir rocks. Ratios between Ca^{2+}, Mg^{2+}, Na^{+}, K^{+}, and Li^{+} cation exchange reactions (i.e. between water and minerals) controlling their concentrations may be determined using cation exchange-based geothermometers. The application of the Na-K geothermometer is based on the ionic exchange, lack of equilibrium between solutes and hydrothermal alteration minerals present in the system, and the enrichment of some cations. For example at equilibrium, ratios of sodium (Na^{+}) and potassium (K^{+}) in a solution are controlled by a temperature dependent exchange reaction in equation (1) by Fournier and Truesdell (1973):

$$NaAlSiO_8 + K^+ = KAlSi_3O_8 + Na^+ \qquad (1)$$

(Albite) (K-feldspar)

The equilibrium (K_{eq}) constant for the reaction is written as equation (2):

$$K_{eq} = \frac{(NaAlSiO_8)(K^+)}{(KAlSi_3O_8)(Na^+)} = [Na^+]/[K^+] \qquad (2)$$

The activity of the chemical species is shown in brackets and the activity of the solid phase is assumed to be unity.

4.3 Multicomponent Geothermometry

Reed and Spycher (1984) in their paper proposed the best estimate of reservoir temperature is attained by considering numerous hydrothermal minerals and the state of equilibrium between specific waters as a function of temperature. Equilibrium constants are both temperature and pressure-dependent, but equilibrium constants for mineral dissolution may often vary strongly with temperature. Saturation indices are the concentration at which dissolved concentrations of mineral components are in saturation with respect to the conditions of the solution. If the saturation index of the solution is greater than zero (>0), then the solution is supersaturated with respect to the mineral solid resulting in the precipitation of that mineral. A saturation index less than zero (<0) means the solution is undersaturated with respect to the mineral, resulting in dissolution. A saturation index of zero indicates equilibrium between the solid and the solution phases with respect to a mineral. The equilibrium between the fluid saturation and the hydrothermal minerals in the reservoir may be determined from the saturation index defined by the equation (3) below:

$$SI = Log\frac{IAP}{K_T} = \frac{Q}{K} \qquad (3)$$

where, *SI* is the saturation index, *IAP* is the product of the ionic activity of the ions, and K_T is the thermodynamic equilibrium constant of the mineral at the discharge temperature of the sample.

TABLE 1: Temperature equations (in °C) for cation geothermometers.

No.	Geothermometer	Equation	Recommended Temperature Range (°C)	Source
1	Na/K	$T_{Na/K} = \left[\frac{1217(\pm 93.9)}{log\left(\frac{Na}{K}\right) + 1.483}\right] - 273.15$	0-250	Fournier (1979)
2	Na/K	$T_{Na/K} = \left[\frac{1319}{log\left(\frac{Na}{K}\right) + 1.699}\right] - 273.15$	25-350	Arnórsson et al.-2 (1983)
3	Na/K	$T_{Na/K} = \left[\frac{1178}{log\left(\frac{Na}{K}\right) + 1.239}\right] - 273.15$	NR	Nieva & Nieva (1987)
4	Na/K	$T_{Na/K} = \left[\frac{1390}{log\left(\frac{Na_m}{K_m}\right) + 1.75}\right] - 273.15$	NR	Giggenbach (1988)
5	Na/K	$T_{Na/K} = \left[\frac{1289(\pm 76}{log\left(\frac{Na}{K}\right) + 0.615}\right] - 273.15$	NR	Verma and Santoya (1997)
6	Na/K	$T_{Na/K} = 733.6 - 770.551[\log\left(\frac{Na_m}{K_m}\right) + 378.189[log\left(\frac{Na_m}{K_m}\right)^2 - 95.753[log\left(\frac{Na_m}{K_m}\right)^3 + 9.5444[log\left(\frac{Na_m}{K_m}\right)^2$	0-350	Arnórsson (2000)
7	Na/K	$T_{Na/K} = \left[\frac{1052}{1 + e\left(1.714\, log\left(\frac{Na}{K}\right) + 0.252\right) + 76}\right]$	100-350	Can (2002)

Concentrations of Na^+ and K^+ are in mg/L or molality (mg/kg) and t is temperature in °C. (For details and references, see Fournier (1979); Arnórsson et al.-2 (1983); Nieva & Nieva (1987); Giggenbach (1988); Verma and Santoya (1997); Arnórsson (2000); and Can (2002). [NR = Not reported.]*

TABLE 2: Temperature equations (in °C) for cation geothermometers.

No.	Geothermometer	Equation	Recommended Temperature Range (°C)	Source
8	Na-K-Ca	$T_{Na-K-Ca} = \left[\frac{1647}{log\left(\frac{Na_m}{K_m}\right) + \beta\left(Log\left(\frac{Ca^{0.5}{}_m}{Na_m}\right) + 2.06\right) + 2.47}\right] - 273.15$	0-250	Fournier and Truesdell (1973)
9	Na-K-Ca (Mg-Corrected)	$T_{Na-K-Ca} = \left[\frac{1647}{log\left(\frac{Na_m}{K_m}\right) + \beta\left(Log\left(\frac{Ca^{0.5}{}_m}{Na_m}\right) + 2.06\right) + 2.47}\right] - 273.15$ (Mg-Correction to this Na-K-Ca geothermometer is provided below)[a]	0-250	Fournier and Potter (1979)
10	Na-K-Ca	$T_{Na-K-Ca} = \left[\frac{1120}{log\left(\frac{Na}{K}\right) + \beta\left(Log\left(\frac{Ca^{0.5}}{Na}\right) + 2.06\right) + 1.32}\right] - 273.15$	0-250	Kharaka and Mariner (1988)
11	Na-K-Mg	$T_{Na-K-Mg} = \left[\frac{2330}{7.35 - log\left(\frac{K^2}{KMg}\right)}\right] - 273.15$	NR	Nieva and Nieva (1987)
12	K^2/Mg	$T_{K/Mg} = \left[\frac{4410}{14.00 - log\left(\frac{K^2}{KMg}\right)}\right] - 273.15$	NR	Giggenbach (1988)

Concentrations of Na^+, K^+, Ca^{2+}, and Mg are in mg/L or molal and t is temperature in °C (For details and references, see Fournier and Truesdell (1973); Kharaka and Mariner (2005); Nieva and Nieva (1987); and Giggenbach (1988). [NR = Not reported.]*

[a]Mg-Correction to the Na-K-Ca geothermometer (Equation 4):

- If $T_{Na-K-Ca}$ is <70°C do not apply correction.
- Calculate R, using equivalents (Molality/Charge) where;

$$R = \frac{Mg}{Mg + Ca + K}(100) \qquad (4)$$

- If R > 50 assume the water is from relatively cool equilibrium conditions with temperatures about equal to the measured water temperature irrespective of the high $T_{Na-K-Ca}$.
- If $T_{Na-K-Ca}$ > 70°C and R<50, use R to determine Δ_{TMg} (Fournier 1979) and subtract Δ_{TMg} from the $T_{Na-K-Ca}$ to get the correct geothermometer temperature.

TABLE 3: Temperature equations for silica geothermometers.

	Geothermometer	Equation	Recommended Temperature Range (°C)	Source
13	Quartz	$T_{Na/K} = \left[\frac{1535}{0.989 - log\ S}\right] - 273.15$	100-275	Truesdell (1976)
14	Quartz (No Steam Loss)	$T_{Na/K} = \left[\frac{1309}{5.19 - log\ S}\right] - 273.15$	70-250	Fournier-1 (1977)
15	Quartz (Maximum Steam Loss-Adiabatic)	$T_{Na/K} = \left[\frac{1522}{5.75 - log\ S}\right] - 273.15$	0-250	Fournier-2 (1977)
16	Quartz	$42.198 + 0.28831S - 3.6686\ x\ 10^{-4}S^2 + 3.1665\ x\ 10^{-7}S^3 + 77.034LogS$	NR	Fournier and Potter (1982)
17	Quartz (Maximum Steam Loss-Adiabatic)	$53.5 + 0.1136 * SiO_2 - 0.5559 * 10^{-4} * {SiO_2}^2 + 0.1772 * 10^{-7}{SiO_2}^3 + 88.39 * LOG(SiO_2$	NR	Arnórsson et al. (1983)
18	Quartz	$55.3 + 0.36598S - 5.3954\ x\ 10^{-4}S^2 + 5.5132\ x\ 10^{-7}S^3 + 74.360\ LogS$	NR	Arnórsson-2 (2000)
19	Quartz	{1175.7(±31.7)]/[4.88(±0.08)-LogS]}-273.15	NR	Verma (2000)
20	Chalcedony	$T_{Chal} = \left[\frac{1112}{4.91 - logS}\right] - 273.15$	25-180	Arnórsson et al. (1983)

For the silica geothermometers (concentrations are molal (mol/L) or ppm), *S* stands for the concentration of SiO_2, *t* is temperature in °C. (For details and references, see Truesdell (1976); Fournier-1 (1977); Fournier-2 (1977); Arnórsson et al. (1983); Verma (2000); Fournier (1977); and Arnórsson et al. (1983)). [NR = Not reported.]*

Silica solubility-based geothermometers are established from experimentally determined variations in the solubility of different silica species (i.e. quartz, chalcedony, cristobalite, amorphous silica, etc.) in water as a function of temperature, pressure, and fluid acidity at the time of mineralization. The increased solubility of quartz and its polymorphs at elevated temperatures has been used extensively as an indicator of geothermal temperatures (Truesdell and Hulston, 1980; Fournier and Potter, 1982). The two silica-based geothermometers most stable at lower temperatures are quartz adiabatic and conductive cooling. Equilibrium with quartz has been found to control the silica concentration in systems above about 180 to 190°C, whereas chalcedony is the controlling phase at lower temperatures (Arnason, 1976). Some boiling occurs in the hot springs at Bath springs with some steam emanating from the surface and bulk rocks, therefore a boiling-corrected geothermometer such as the Quartz maximum steam loss (Fournier, 1977) was one of several geothermometers applied to the hot spring waters. Quartz geothermometers are susceptible to various steam losses due to lower silica concentrations and tend to underestimate the reservoir temperature. Temperature can be derived from the following relationships for equilibrium with these silica polymorphs from 0 to 250°C, where Si concentrations are in ppm (Fournier, 1981).The basic reaction for silica dissolution in water is shown in equation (5):

$$SiO_{2(qtz)} + 2H_2O = H_4SiO_4 \quad (5)$$

The saturation index (Log *Q/K*) was calculated for minerals assumed to be relevant like quartz, chalcedony, calcite, aragonite, dolomite, siderite, hematite, goethite, and talc for all water samples using the United States Geological Survey's PHREEQC package (Parkhurst and Appelo, 1999) modeling code interfaced with AquaChem. PHREEQC program is based on an ion-association aqueous model that has capabilities for speciation, saturation-index calculations, and inverse modeling. It uses available chemical analyses assumed to be representative of the chemical evolution of groundwater along a given flow path and attempts to both identify and quantify the heterogeneous reactions that may have been responsible for that chemical evolution (Konikow and Glynn, 2005). Hence, the Log(Q/K) value for each mineral provides a measure of the proximity of the aqueous solution components to attaining equilibrium with the mineral. A multicomponent approach to geothermometry involved using full chemical analysis of the spring water samples to compute the saturation indices Log(Q/K) of the reservoir minerals over a range of temperatures (25-220°C). The saturation indices were graphed as a function of temperature and the clustering of Log(Q/K) curves near zero at any specific temperature for a group of minerals) used to infer the reservoir temperature. Minerals that equilibrate with the fluid will intersect or converge where the Log (Q/K) equals zero for at the same temperature (e.g. 80ºC), whereas other minerals will not intersect it (Reed and Spycher, 1984). The characteristic convergence of Log (Q/K) versus T(°C) curves for all minerals that are in contact with the solution (equilibrium assemblage) to zero at the same temperature of equilibration is the basis for the multicomponent approach to geothermometry. The mixing of solutions of varied composition with geothermal fluids at equilibrium with hydrothermal minerals causes a shift in the position in which the minerals are apparently at equilibrium to a lower log through dilution. Therefore, if a group of minerals converges to equilibrium at a particular temperature, this temperature corresponds to the most likely reservoir temperature, or at least the temperature of the source aquifer, for the particular water considered (Reed and Spycher, 1984).

5. RESULTS AND DISCUSSION

5.1 Geothermometric Modeling

Geochemical modelling using PHREEQC interfaced with AquaChem enabled the prediction of the saturation state of minerals and indicated the dissolution and precipitation reactions occurring in the emergent thermal spring waters with the reservoir rocks. Thermodynamic calculations performed shows that the saturation index calculations based on minerals are presumed to precipitate, dissolve or are at equilibrium with respect to the exposed rocks (Figure 6-7). The steam heated, hot spring samples (BTHN and BTHS) are undersaturated with respect to the minerals dolomite, anhydrite, gypsum, siderite, and halite and is therefore capable of

dissolving these minerals. The saturation indices of quartz, chalcedony, and calcite in solutions have equilibrated and quartz is the more stable silica phase in the waters (SI = 0.4970-0.6114) over the temperature range 20 to 220°C (Figure 6-7). This suggests that the amorphous and opaline silica phases do exert control on the silica phases of these waters. Open, brittle fractures form localized low-pressure zones (i.e. spaces) in which any hydrothermal fluid in the immediate area will immediately migrate and precipitate minerals. BTHN and BTHS are oversaturated with respect to goethite, hematite and talc (Figure 6-7). This may be explained by the elevated pH, Fe concentrations, and low Eh values that favor the precipitation of Fe minerals. For alkaline thermal waters (pH>7.3), PHREEQC predicted precipitation of goethite and hematite, which is reflected in the low concentrations of iron (0.53 to 0.58 mg/L) and aluminum (0.24 mg/L) in the waters. It must be noted that dilution by shallow subsurface mixing and re-equilibration along the flow path lowers calculated temperatures. Clustering of quartz, chalcedony, and calcite occurs near zero between over a specific temperature range of 80-102°C (Figure 6-7). SI values for goethite, hematite, dolomite, and siderite plot at their minimum at 100°C. SI values for talc appear to level off from 100°C to 200°C onwards.

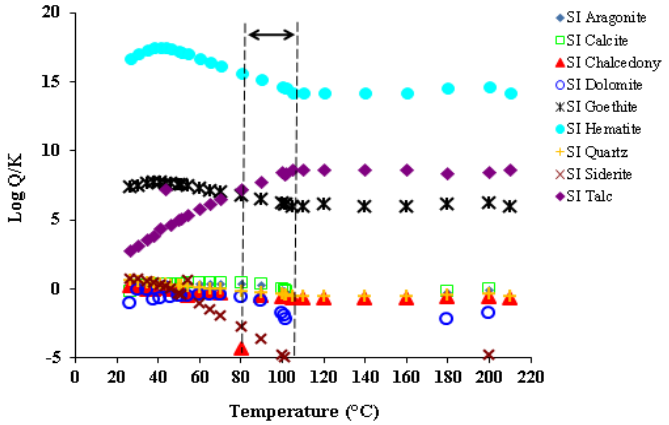

Figure 6: Multicomponent geometry using the BTHN sample with saturation indices [Log (Q/K)] of several minerals graphed as a function of temperature over a range of 20-210°C. The 80-102°C range between the dashed vertical lines indicates the estimated reservoir temperatures. For systems at 'full equilibrium', the equilibrium temperature is normally inferred from the temperature at which the indices converge at the minimum.

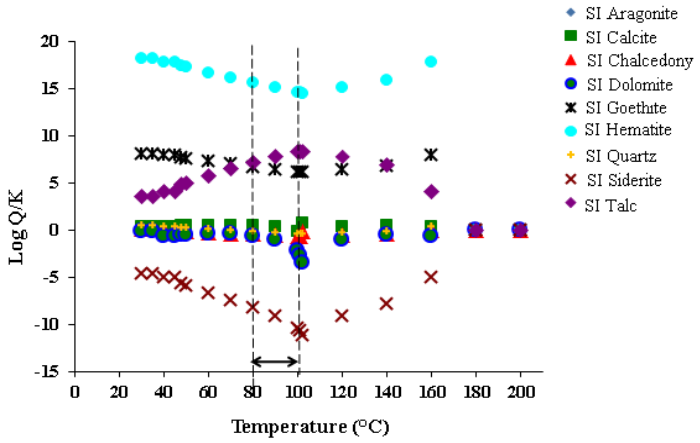

Figure 7: Multicomponent geometry using the BTHS sample with saturation indices Log(Q/K)] of several minerals graphed as a function of temperature over a range of 20-210°C. The 80-102°C range between the dashed vertical lines indicates the estimated reservoir temperatures. For systems at 'full equilibrium', the equilibrium temperature is normally inferred from the temperature at which the indices converge at the minimum.

The dispersion and lack of the Log(Q/K) curves total convergence to zero for several hydrothermal minerals suggest the existence of a partial and not 'full equilibrium' which is the result of mixing, boiling, and dilution during ascent. This is in agreement with the plot of BTHN and BTHS samples in the 'partial equilibrium' region of the Giggenbach (1988) Na-K-Mg geoindicator shown in Figure 8. The coexistence of hematite, goethite, talc and dolomite in these fluids imply interaction with hydrothermal alteration of metamorphic wall rocks. If the geothermal fluid has boiled before it is sampled, since the formation of the residual aqueous solution and a simultaneous increase in pH, both tend to cause the supersaturation of certain mineral phases (e.g. calcite and hematite). These factors will lead to complex changes in the various apparent equilibrium mineral or solution temperatures and will result in varied performance of both cation exchange and silica solubility geothermometers. Physical processes that affect water-mineral equilibria can result in unreliable temperature predictions include boiling, mixing with cold water and steam vapor fractions (Verma, 2000; Verma, 2015).

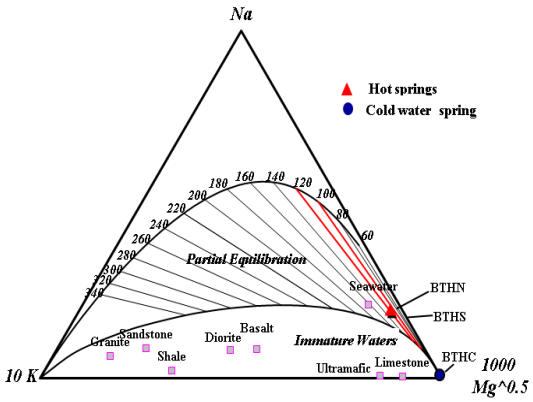

Figure 8: Ternary diagram for evaluating Na/K, K/Mg1/2 temperatures in geothermal waters (modified from Giggenbach, 1988). Spring samples from this site are plotted with their feature identification numbers. Red represents hot springs (BTHN, BTHS = >30°C) and blue triangle represents cold springs (BTHC = ≤ 30°C).

5.2 Comparison of Cation and Silica Geothermometers

The geothermometers are expected to provide a minimum estimate of the highest temperature reached in the geothermal system. Na-K, Na-K-Ca and quartz solubility temperatures were calculated for the Bath hot spring water samples. The results of the temperatures estimated using the geothermometric equations are presented in Table 4.

TABLE 4: Selected Geothermometers.

	Geothermometer	Temperature Range (°C)	Sample BTHN	Sample BTHS-1	Sample BTHS-2
1	Na/K	Fournier (1979)	84	83	102
2	Na/K	Arnórsson et al.-2 (1983)	89	88	107
3	Na/K	Giggenbach et al. (1988)*	99	101	118
4	Na/K	Verma and Santoyo (1997)	85	87	104
5	Na/K	Arnórsson (2000)	84	85	88
6	Na/K	Can (2002)	103	103	112
7	Na-K-Ca (Mg-Corrected)	Fournier and Potter (1979)	213	211	238
8	Na-K-Ca	Fournier and Truesdell (1973)	136	264	223
9	Na-K-Ca	Kharaka and Mariner (1989)	240	236	281
10	Na-K-Mg	Nieva and Nieva (1987)	86	84	97
11	K^2/Mg	Giggenbach et al. (1988)	64	59	70
12	Quartz	Truesdell (1976)	86	84	84
13	Quartz	No Steam Loss, Fournier (1977)	81	79	81
14	Quartz	Maximum Steam Loss, Fournier (1977)	84	83	83
15	Quartz	Fournier & Potter (1989)	81	81	81
16	Quartz	Fournier & Potter (1989)	80	79	79
17	Quartz	Arnórsson (2000)	66	65	65
18	Quartz	Verma (2000)	72	74	74
19	Chalcedony	Arnórsson et al. (1983)	65	67	67

The Na/K geothermometer is less affected by dilution or steam loss given that it is based on a ratio and re-equilibration is slower than that of the silica-quartz geothermometer. It is demonstrable to apply the Na/K or the Na-K-Ca geothermometer to alkaline waters as they would be in equilibrium with feldspars. Ca^{2+}, Li^{+} and Mg^{2+} are normally present at low concentrations in geothermal waters. The Na–K–Mg ternary diagram is an empirical geothermometer first proposed by Giggenbach (1988) and shown in Figure 8. Besides conveniently allowing easier assessment of inter-relations of Mg and Na/K geothermometers in a unique graph, it allows the distinction between 'suitable' or 'unsuitable waters' for the application of ionic solute geothermometers as it divides thermal fluids into three fields: '*fully equilibrated*', '*partially equilibrated*', and '*immature waters*' as a function of their Na, K and Mg content(s). The Bath data were plotted on a version of the diagram by Giggenbach and Corrales, 1992 that is more suitable for low-temperature geothermal systems (i.e. in the range of 20-220°C) and later modified by Powell and Cummings (2010). The hot spring samples BTHN and BTHS plot in the 'partially equilibrated' field indicating a high degree of mixing with either non-equilibrated or non-thermal waters (Figure 8). The cold water sample BTHS falls in the immature waters' field as is expected (Figure 8).

The extent of fluid mixing on the evolution of BTHN and BTHS hot spring samples is demonstrated in Figures 8-11. The 10Mg/(10Mg + Ca) Vs. 10K/(10K + Na) plot in Figure 9 shows both samples plot below the 'full equilibrium' line and away from the region of 'seawater mixing' indicating dissolution of the wall rock exclusive of the influence or any mixing with seawater.

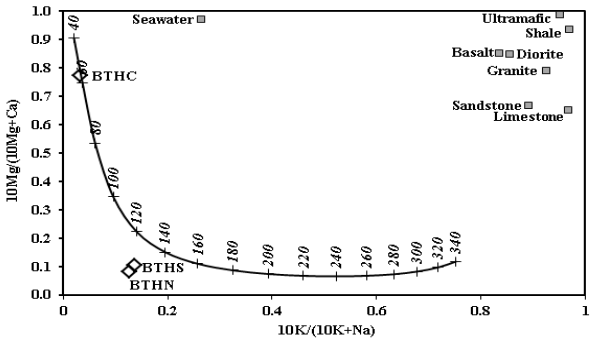

Figure 9: Diagram showing 10Mg/(10Mg + Ca) vs. 10K/(10K + Na) plots for the thermal, low-temperature and cold mineral springs in (mg/kg).

The Na-K-Ca geothermometer is sensitive to variations in PCO_2 being that Ca^{2+} is a constituent of calcite (a mineral containing CO_2 and involved in hydrothermal alteration systems). CO_2 is likely a major component of most geothermal fluids; therefore, it is expected to contain non-equilibrium amounts and allow minor amounts of Ca^{2+}, K^+, Mg^{2+} to adjust to the prevailing conditions of temperature and partial pressure. An intricate correlation exists among PCO_2 and the CO_2 contents of the coexisting liquid and vapor phases. This is demonstrated by the graph in Figure 10 (Giggenbach 1986). Values that plot as in the case of BTHN and BTHS above the line representing "CO_2 partial pressures for a full equilibrium" may be the result of isothermal boiling associated with dilution and lower than equilibrium partial pressures of CO_2 (Figure 10). Data points that fall below the "PCO_2 partial pressures-full equilibrium line" correspond to the composition of immature fluids with higher CO_2 concentrations rather than at full equilibrium and are reactive with respect to hydrogen metasomatism (Giggenbach 1988). The amount of conductive heat loss of ascending geothermal waters is proportional to the distance travelled and inversely proportional to the flow rate. Geotemperatures estimated from silica geothermometry may be lower due to the presence of high salinity fluids that alter quartz solubility; the effects of steam separation that may precipitate silica; and the effect of pH on quartz solubility or dilution due to shallow mixing with cold meteoritic water. Concordance between estimated temperatures modeled by the coupled geothermometers using a cross plot of SiO_2 vs. Log(K^2Mg) modified from Giggenbach, 1988 in 2010 by Powell and Cummings in their Liquid Analysis Spreadsheet indicates a reservoir temperature of 75°C (Figure 11).

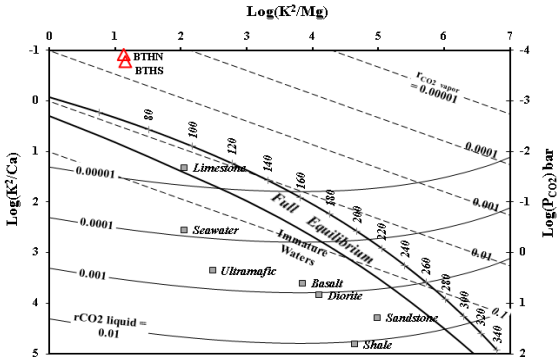

Figure 10: Evaluation of CO_2 partial pressures in the Bath geothermal system by use of K, Mg, and Ca contents of their discharge (Giggenbach 1988).

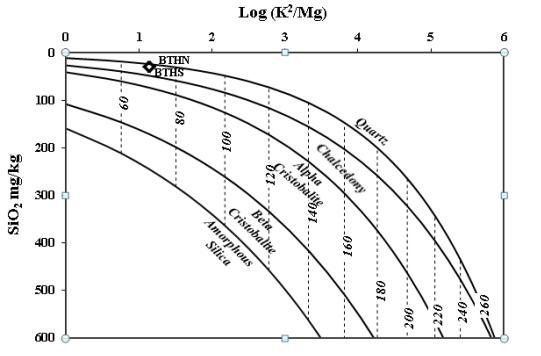

Figure 11: Cross plot of K^2/Mg versus Silica geothermometer results for Bath hot springs.

It is well-noted in the literature that estimates of reservoir temperatures computed from the cation geothermometers for each sample are generally higher than those of silica geothermometers. Geotemperatures estimated for the Bath hot springs vary between 84°C to 118°C for Na/K; 80°C to 97°C for Na-K-Mg; 86°C to 238°C for Na-K-Ca; 86°C to 97°C for chalcedony; and 65°C to 86°C for quartz the temperatures (Table 3). The results of the Na-K geothermometer in (Figure 7-8) may be explained by mixing geothermal

fluids and steam in addition to CO_2 degassing during their ascent to the surface (Pang and Reed, 1998), but with no significant change in the Na/K ratio (Pope et al.1987). Low geotemperatures estimated using the K^2/Mg geothermometer or any combination (Figure 10-11) may have resulted from dilution of saline geothermal fluids by meteoritic water. Verma (2015) and Torres-Alvarado et al. (2012) point out some limitations/oversights of the application of average temperatures for the Na/K and silica solubility geothermometers to high enthalpy geothermal systems. In their report they noted differences in temperature/pressure result in substantial differences in the calculated reservoir fluid characteristics (e.g. temperature) and negative or near zero vapor-fraction for low enthalpy wells. Verma (2015) raises several valid points regarding the use of the Na/K geothermometer and his abandonment of it on the basis of thermodynamics and the laws of chemistry. While the arguments are plausible in regards to Los Azufres, Los Humeros, Cerro Prieto and other such high enthalpy systems with temperatures in excess of 300 °C, the Bath geothermal reservoir (Jamaica) is low enthalpy system with temperatures reasonably estimated at 80-120°C. B and Cl isotope geothermometers seemed to have provided comparable estimates of temperature for the Los Humeros geothermal field (Mexico) that has high steam/vapor fractions. It is reported throughout the literature that the Na/K geothermometer appears to be less affected by fluid mixing and boiling than the silica geothermometer and it may be reasonable to assume that minimum re-equilibration may have occurred with the wall rocks during ascent. The true prevailing conditions of the system are unknown and data provided from boreholes or wells allow a better understanding of the prevailing thermodynamics (i.e. temperature, pressure, enthalpy, entropy, vapor fraction) of geothermal systems. Simulations of multicomponent geothermometry show that the concentration of species such as Na, K, and SiO_2 are less sensitive to re-equilibration compared to species like Al^{3+} and Mg^{2+} (Peiffer et al., 2014). It is noted that solute geothermometers based on the abovementioned species give reasonable reservoir temperature in most cases except under conditions of dilution or mixing with saline water (Peiffer et al., 2014). Furthermore, it must be borne in mind that geothermometers reflect a steady-state condition that exists at higher temperatures between the circulating geothermal fluids and reservoir rocks and many geothermal systems may never reach equilibrium (Barton, 1984). Therefore, cation and silica geothermometers are used here with extreme caution. The Na/K geothermometer compared to the silica geothermometer (Figure 12) may be assumed to be more representative of reservoir conditions (e.g. temperature) in the deeper parts of the geothermal system as fluids may equilibrate at lower temperatures and shallow depths during a slow ascent depending on the system hydrology.

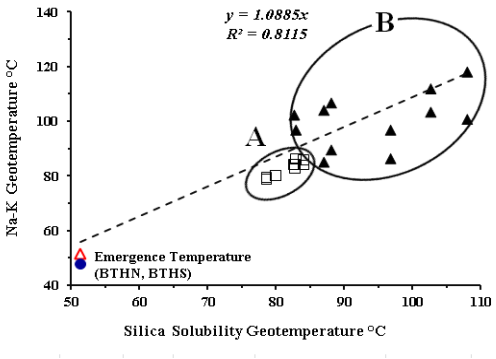

Figure 12: Estimated temperatures from quartz geothermometers (Verma, 2000; Fournier and Potter, 1989; Fournier, 1977; Fournier, 1977; and Truesdell, 1976) vs. Na/K geothermometer (Can, 2002; Arnórsson et al. (2), 2000; Verma and Santoyo, 1997; Giggenbach, 1988; and Fournier, 1979).

Other cation geothermometers appeared to provide less reliable estimations of reservoir temperatures. The K^2/Mg, Na/Li underestimated the reservoir temperatures whereas the Na-K-Ca and Na-K-Ca-Mg appeared to overestimate the temperature. The K^2/Mg geothermometer was applied with a lower confidence level as the reservoir K^2/Mg ratios are scattered with respect to Mg-chlorite-K-mica-K-feldspar-quartz equilibria. Overall, the graphs and empirical results implies a good agreement exists between the temperatures calculated from the Na/K and Na-K-Mg geothermometers and may be fairly reliable. Based on the estimated geotemperatures of the Bath, the reservoir temperatures estimated from emergent hot spring waters are low (<180°C) and are indicative of a low enthalpy system. The interpretation of the results so far was assessed by taking into account the characteristics of the rugged terrain and the processes that can occur during the movement from the deep reservoir to the surface.

5.3 Estimation of Depths to the Geothermal Reservoir

Circulation depths in geothermal systems may be estimated by comparing the equilibrium temperature of thermal springs with the local or regional geothermal gradient which varies from place to place. Complex geothermal gradients may develop in response to deep circulation systems based on models as depth-integrated gradients vary purely from conductive heat flow by up to approximately 20% (Lopez and Smith (1995). It must be noted that the circulation depth of a geothermal system may also be related to the depth of the fault plane below the zone of meteoritic recharge as faults act as effective conduits for fluid flow along the fault and may also be effective barriers to fluid flow across the fault (Lopez and Smith (1995). The most reliable reservoir temperatures are provided by direct borehole temperatures measurements from exploratory wells. However, borehole data are not yet available to provide more detailed information about the flow path of the rugged terrain at Bath and the use of emergence temperatures makes it difficult to accurately predict the geothermal gradient. Therefore, using the geothermal gradients for the Caribbean at 25°C/km - 30°C/km, a similar range of geothermal gradients was assumed for the Bath region. Wishart (2013) estimated the depth to the Bath geothermal reservoir ranges from 1.0 to 1.8 km based on the assumption that the average

geothermal gradient was 25°C/km - 30°C/km. However, these results are minimum estimates and do not preclude the possible existence of deeper flow systems.

5.4 Uses of Low Enthalpy Geothermal Water

Geothermal energy has been used for heating, industry, and the generation of electricity. The water from Bath hot springs has been primarily used for balneological or therapeutic (spa) treatments for locals and tourists. Low enthalpy geothermal fluids (50-150°C) have been used for agriculture, fruit drying, aquaculture, horticulture, space heating, spas, paper manufacturing and other applications (Fridleifsson, 1998). This geothermal fluid can be used in an integrated system which includes district and greenhouse heating. Binary cycle power plants are operable with temperatures as low as 57°C (Erkan et al. 2008). These are lower than the reservoir temperatures estimated for the Bath geothermal reservoir. Recently, the Bath hot springs has been identified as one of six potential sites for geothermal power development of a 15MW plant in Jamaica starting 2016.

5.5 Recommendations for Future Investigations

The next phase of this investigation will include geothermal exploration well drilling, BHT measurements, determination of the local geothermal gradient, geophysical surveys (including self potential, audiomagnetotellurics (AMT), and seismic tomography), and hyperspectral imaging of hydrothermal alteration for the development of geothermal resources. It is recommended that for future geothermal prospecting and exploration, that the static formation temperatures be used as they are expected to be more representative of the equilibrium reservoir temperature that governed the initial water–rock interaction process. Bottom-hole temperatures are unevenly perturbed by the drilling operations.

6. CONCLUSION

A range of several widely used solute geothermometers (Na/K, the Giggenbach Na-K-Mg, K^2/Mg, Na-K-Ca, silica-quartz and silica-chalcedony) were used to estimate the geotemperatures of the Bath geothermal reservoir from water samples collected at the ground surface. A preliminary evaluation of the geothermometers estimated geotemperatures over a range of 64-281°C. The temperatures calculated from the silica geothermometers were generally lower than those calculated from the cation geothermometers. These lower estimates of reservoir temperature may be due loss of silica during ascent, degassing by CO_2, conductive cooling, mixing with saline waters, dilution, or meteoritic recharge. The highest reservoir temperature provided by the quartz (maximum steam loss) geothermometer is 84°C (Fournier (2), 1977). According to Na/K geothermometers, reservoir temperatures of thermal waters range from 84°C to 118°C. Geotemperatures for the Na-K–Mg geothermometers ranged from 86°C to 97°C. Results provided from the multicomponent geothermometric modeling of variation of Log(Q/K) over a range of temperatures (using PHREEQC interfaced with AquaChem) compared with solute geothermometers show a temperature cluster of around 80-102°C. The more widely used Na/K, and Na-K-Mg geothermometers appeared to provide more consistent results and are probably closer to the temperature of the Bath geothermal reservoir. Analyses of data provided by chemical geothermometric equations, ternary diagrams, graphs, multicomponent geothermometry indicate the reservoir temperatures of the Bath geothermal system can reasonably reach as much as 118°C. Multicomponent geothermometry coupled with graphical hydrogeochemical analyses provided a useful approach to reconstruct the fluid composition at depth and provide preliminary estimates of the reservoir temperature. The geothermal resource at Bath is considered a low enthalpy type and is clearly related to the tectonic uplift and structural setting of the Blue Mountain Inlier. Fissures and faults associated with the reservoir rocks permit the infiltration of meteoritic waters that are heated up at depth with increasing geothermal gradient and ascend to the surface via convection. The results of this investigation have laid the groundwork for further exploration for the development of geothermal resources with exploratory geothermal well drilling, geophysical investigations and hyperspectral imaging.

ACKNOWLEDGEMENTS

The author is grateful to Reviewer No. 1 (an anonymous reviewer), for the constructive review of the original manuscript, helpful comments, and suggestions. The author wishes to thank Dr. Roland Horne, Thomas Davies Barrow Professor, School of Earth Sciences and Senior Fellow at the Precourt Institute for Energy, Stanford University, California, USA for insightful direction on relevant updates in the literature. Both their efforts assisted tremendously in the enhancement of the quality of this manuscript. This investigation was partially funded by National Science Foundation (NSF) ADVANCE LEADER minigrants Grants No. 8449 and No. 8451 from Wright State University and Central State University, Ohio.

REFERENCES

Arnason, B.: Ground Water Systems in Iceland Traced by Deuterium, *Societas Scientiarum Islandica,* **42**, (1976), 236.

Arnórsson, S. (Ed.): Isotopic and Chemical Techniques in Geothermal Exploration, Development and Use: Sampling Methods, Data Handling, Interpretation, International Atomic Agency, Vienna, Austria, (2000), 351.

Arnórsson, S., Fridriksson, T., Gunnarsson, I.: Gas Chemistry of the Krafla Geothermal Field, Iceland. In G.B. Arehartand J.R. Hulston (eds.), *Water-Rock Interaction*, (1998), 613-616. Rotterdam: Balkema.

Arnórsson, S.: The Use of Mixing Models and Chemical Geothermometers for Estimating Underground Temperatures in Geothermal Systems, *Journal of Volcanology and Geothermal Research,* **23**, (1985), 299-335.

Arnórsson, S.: Chemical Equilibria in Icelandic Geothermal Systems: Implications for Chemical Geothermometry Investigations, *Geothermics*, **12**, (1983), 119-128.

Barton, P. B., Jr.: High Temperature Calculations Applied to Ore Deposits-Chapter 14, In: Henley, R.W., A.H. Truesdell, and P.B. Barton, Jr., (Eds.), Fluid-Mineral Equilibria in Hydrothermal Systems, *Reviews in Economic Geology*, **1**, (1984), 191-201.

Battistel, M., Barbieri, M., Hurwitz, S., Eavans, W., Chiodini, G.: Multicomponent Geothermometry Applied to Medium-Low Enthalpy Carbonate-Evaporite Geothermal Reservoir, *Geophysical Research Abstract*s, **16**, (2014), European Geosciences Union, European General Assembly.

Can, I.: A New Improved Na/K Geothermometer By Artificial Neural Networks, *Geothermics*, **31**, (2002), 751-760.

Chan, L., Geiskes, J. M., You, C., Edmond, J. M.: Lithium Isotope Geochemistry of Sediments and Hydrothermal Fluids of the Guaymas Basin, Gulf of California, *Geochimica et Cosmochimica Acta*, **58**, (1994), 4443-4454.

Dulanya, Z., Morales-Simfors, N., Sivertun, A.: Comparative Study of the Silica and Cation Geothermometry of the Malawi Hot Springs: Potential Alternative Energy Source, *Journal of African Earth Sciences*, **57(4)**, (2010), 321-327.

Ellis, A.J., Mahon, W.A.J.: Chemistry and Geothermal Systems, Academic Press, New York, (1977), 392.

Erkan, K., Holdmann, G., Benoit, W., and Blackwell, D.: Understanding the Chena Hot Springs, Alaska Geothermal System Using Temperature and Pressure Data, *Geothermics*, **37(6)**, (2008), 565-585.

Fournier, R.O.: Lectures on Geochemical Interpretation of Hydrothermal Waters: United Nations University Geothermal Training Programme, Reykjavik, Iceland, Report 10, (1989), 73.

Fournier, R.O.: A Revised Equation for the Na/K Geothermometer, *Geothermal Resources Council Transactions*, **3**, (1979), 221-224.

Fournier, R.O.: Chemical Geothermometers and Mixing Models for Geothermal Systems, *Geothermics*, **5**, (1977), 41-50.

Fournier, R.O.: Silica in Thermal Water: Laboratory and Field Investigations, In: Proceedings of the International Symposium on Hydrogeochemistry and Biochemistry, Japan, (1970), **1**, Washington DC, Clark, (1973), 122-139.

Fournier, R.O., Potter, R.W.: A Revised and Expanded Silica (Quartz) Geothermometer, *Geothermal Resources Council Bulletin*, **11**, (1982), 3-12.

Fournier, R.O., Potter, R.W.: Magnesium Correction to the Na-K-Ca Chemical Geothermometer, *Geochimica et Cosmochimica Acta*, **43**, (1979), 1543–1550.

Fournier, R.O., Truesdell, A.H: An Empirical Na-K-Ca Geothermometer for Natural Waters, *Geochimica et Cosmochimica Acta*, **37(5)**, (1973), 1255-1275.

Fridleifsson, I.: Geothermal Direct Use Around the World, *Geothermal Resources Council, Bulletin*, **27(8)**, (1998).

Gherardi, F., Spycher, N.: Application of Integrated Multicomponent Geothermometry at the Chachimbiro Thermal Area, a Difficult Geothermal Prospection Case, *Proceedings*, the 25th Workshop on Geothermal Reservoir Engineering, (2013), Stanford University, Stanford, CA, SGP-TR-202.

Giggenbach, W. F.: Geothermal Solute Equilibria, Derivation of the Na-K-Mg-Ca Geoindicators, *Geochimica et Cosmochimica Acta*, **52**, (1988), 2749-2765.

Giggenbach, W. F.: Graphical Techniques for the Evaluation of Water/Rock Equilibration Conditions By Use of Na. K, Mg, and Ca-Contents of Discharge Waters*, Proceedings*, the 8th New Zealand Geothermal Workshop (1986).

Giggenbach, W. F., Corrales, R.: The Isotopic and Chemical Composition of Water and Gas Discharges from the Guanacaste Geothermal Province, Costa Rica, *Applied Geochemistry*, **7**, (1992), 309-332.

Hastie, A. R., Ramsook, R., Mitchell, S. F., Kerr, A. C., Millar, I. L, Mark, D.: Geochemistry of Compositionally Distinct Late Cretaceous Back-Arc Basin Lavas: Implications for the Tectonomagnetic Evolution of the Caribbean Plate, *Journal of Geology*, **118**, (2010), 655-676.

Hastie, A. R., Kerr, A. C., Mitchell, S. F., Millar, I. L., Mark, D.: Geochemistry and Petrogenesis of Cretaceous Oceanic Plateau Lava in Eastern Jamaica, *Lithos*, **101**, (2008), 323-343.

Hylton, H. A.: The Mineral Springs of Jamaica, Geological Survey Division Bulletin **11**, Ministry of Mining, Energy and Tourism, Jamaica, (1987), 1-69.

Kerr, A.C. and Tarney, J.: Tectonic Evolution of the Caribbean and Northwestern South America: the Case for Accretion of Two Late Cretaceous Oceanic Plateaus, *Geology*, **33**, (2005), 269–272.

Kharaka Y.K, Mariner R. H.: Chemical Geothermometers and Their Application to Formation Waters from Sedimentary Basins. In: Naser N. D., McCulloh, T. H. (Eds.), Thermal History of Sedimentary Basins; Methods and Case Histories, Springer, New York, (1989), 99–117.

Konikow, L. F., Glynn, P. D.: Modeling Groundwater Flow and Quality, In: Impacts of the Natural Environment on Public Health, O. Selinus, B.J. Alloway, J.A. Centeno, R.B. Finkelman, R. Fuge, U. Lindh, P. Smedley (Eds.), Elsevier Academic Press, (2005), 737–765.

Lopez, D. L., Smith, L.: Fluid Flow in Fault Zones: Analysis of the Interplay of Convective Circulation and Topographically-Driven Groundwater Flow, *Water Resources Research*, **31**, (1995), 1489-1503.

Mann, P., Demets, C., Wiggins-Grandison, M.: Towards a Better Understanding of the Late Neogene Strike-Slip Restraining Bend in Jamaica: Geodetic, Geological and Seismic Constraints. Geological Society, London, Special Publications, **290**, (2007), 239-253, doi:10.1144/SP290.8.

Mann, P., Draper, G., Burke, K.: Neotectonics of a Strike-Slip Restraining Bend System, Jamaica. In: K. Biddle, and N. Christie-Blick, (Eds.) Strike-Slip Deformation, Basin Formation, and Sedimentation, *SEPM Special Publications*, **37**, (1985), 211–226.

Nieva, D., Nieva, R.: Developments in Geothermal Energy in Mexico-Part Twelve. A Cationic Geothermometer For Prospecting of Geothermal Resources, *Heat Recovery Systems*, **7(3)**, (1987), 243-258.

Pang, Z. H., Reed, M. H.: Theoretical Chemical Thermometry on Geothermal Waters: Problems and Methods, *Geochimica et Cosmochimica Acta*, **62**, (1998), 1082-1091.

Parkhurst, D. L., Appelo, C. A. J.: User's Guide to PHREEQC (Version 2): A Computer Program for Speciation, Batch Reaction, One Dimensional Transport and Inverse Geochemical Calculations, U. S. Department of the Interior, US Geological Survey. Water Resources Investigation Report, (1999), 99-4259.

Peiffer, L., Wanner C., Spycher, N., Sonnenthal, E. L., Kennedy, B. M., and Iovenitti, J.: Optimized Multicomponent VS. Classical Geothermometry: Insights from Modeling Studies at the Dixie Valley Geothermal Area, *Geothermics*, **51**, (2014), 154-169.

Piper, A. M.: A Graphic Procedure in the Geochemical Interpretation of Water Analyses, *American Geophysical Union Transactions*, **25**, (1944), 914-923.

Pope, L.A., Hajash, A., Popp, R.K.: An Experimental Investigation of the Quartz, Na-K, Na-K-Ca Geothermometers and the Effects of Fluid Composition, *Journal of Volcanology and Geothermal Research*, **31(1-2)**, (1987), 151-161.

Powell, T., Cumming, W.: Spreadsheets for Geothermal Water and Gas Geochemistry, *Proceedings*, 35th Workshop on Geothermal Reservoir Engineering, Stanford University, Stanford, CA, (2010), SGP-TR-188.

Reed, M. H., Spycher, N.: Calculation of pH and Mineral Equilibria in Hydrothermal Waters with Application to Geothermometry and Studies of Boiling and Dilution, *Geochimica et Cosmochimica Acta*, **48**, (1984), 1479-1492.

Santoyo, E and Díaz-Gonzaleź: A New Improved Proposal of the Na/K Geothermometer to Estimates Deep Equilibrium Temperatures and Their Uncertainties in Geothermal Systems, *Proceedings*, the World Geothermal Congress (2010), April 25-29, 2010, Bali, Indonesia.

Schoeller, H.: La Classification Géochemique des eaux, IASH Publication **65**, General Assembly of Berkeley, **4**, (1963), 16-24.

Spycher, N., Peiffer, L., Sonnenthal, E. L., Salda, G., Reed, M. H., Kennedy, B. M.: Integrated Multicomponent Solute Geothermometry, *Geothermics*, **51**, (2014), 113-123.

Torres-Alvarado, I. S., Verma, M. P. Opondo, K., Nieva, D., Haklidir, F. T., Santoyo, E., Barragán, R. M., Arellano, V.: Estimates of Geothermal Reservoir Fluid Characteristics: GeoSys. Chem and WATCH, *Revista Mexicana de Ciencias Geológicas*, **29(3)**, (2012), 713-724.

Truesdell, A. H., Hulston, J. R.: Isotopic Evidence on Environments of Geothermal Systems. In: P. Fritz and J. Ch. Fontes (Eds.), Handbook of Environmental Isotope Geochemistry, **1**, The Terrestrial Environment, Amsterdam, (1980), 179-226.

Truesdell, A.H.: Summary of Section III - Geochemical Techniques in Exploration, *Proceedings*, the Second United Nations Symposium on the Development and Use of Geothermal Resources, San Francisco, CA, **1**, (1976), 1iii-1xiii.

Verma, M. P.: Chemical and Isotopic Geothermometers to Estimate Geothermal Reservoir Temperature and Vapor Fraction, *Proceedings*, the World Geothermal Congress (2015), Melbourne, Australia, #14125.

Verma, M.P.: Cation Exchange Geothermometry: A Critique, *Geotermia*, **25**, (2012c), 53-56.

Verma, M. P.: Geochemical Evidence for a Lithospheric Source for Magmas from Los Humeros Caldera, Puebla, Mexico, *Chemical Geology*, **164**, (2000), 35-60.

Verma, M. P.: Limitations in Applying Silica Geothermometers from Geothermal Reservoir Evaluation, *Proceedings*, the 25th Workshop on Geothermal Reservoir Engineering, Stanford University, Stanford, CA, (2000), SGP-TR-165.

Verma, M.P., Santoyo E.: New Improved Equations for Na/K, Na/Li and SiO_2 Geothermometers by Outlier Detection and Rejection, *Journal of Volcanology and Geothermal Research*, **79(1-2)**, (1997), 9-24.

Wiggins-Grandison, M., Atakan, K.: Seismotectonics of Jamaica, *Geophysical Journal International*, **160(2)**, (2005), 573-580, doi: 10.1111/j.1365-246X.2004.02471.

Wiggins-Grandison, M., Kebeasy, T. R. M., Husebyei, E. S.: Enhanced Earthquake Risk of Kingston Due to Wave Field Excitation in the Liguanea Basin, Jamaica, *Caribbean Journal of Earth Science*, **37**, (2003), 21-32.

Wishart, D. N.: Geothermometry and Shallow Circulation of a Low Enthalpy System: The Bath Geothermal System, Jamaica, West Indies, *Proceedings*, the 38th Workshop on Geothermal Reservoir Engineering, Stanford University, Stanford CA, (2013), SGP-TR-198.